



Research on High Precision Adaptive Phasor Measurement Algorithm Based on Taylor Series and Discrete Fourier Transform

Guangfu Wang¹, Huanxin Guan², Peng Jin³, and Yan Zhao²(✉)

¹ School of Electric Power, Shenyang Institute of Engineering,
Shenyang 110136, Liaoning, China
m18265537369@163.com

² School of Renewable Energy, Shenyang Institute of Engineering,
Shenyang 110136, Liaoning, China

³ State Grid Liaoning Electric Power Co., Ltd.,
Shenyang 110136, Liaoning, China

Abstract. The application of HVDC power transmission, flexible ac power transmission and large-scale grid connection of new energy have introduced a large number of power electronic equipment to the power grid. This results in frequent subsynchronous oscillations, and the harmonic disturbance of power grid presents a broadband trend, which seriously affects the accuracy of phasor measurement. To solve the problem that the traditional phasor algorithm can not satisfy the demand of precision and speed in the dynamic process, this paper proposes a comprehensive adaptive phasor algorithm based on Taylor series and discrete Fourier transform (DFT). For steady state and dynamic state, the time domain algorithm and the frequency domain algorithm are designed respectively. Specifically, the time-domain algorithm USES two adjacent data Windows for DFT analysis, and is simplified according to specific accuracy requirements to calculate the frequency and phasor. The Taylor series expansion of the power signal model is carried out by the frequency domain algorithm, and the phasor, frequency and frequency change rate are calculated by the fundamental wave and each harmonic content of a data window. Finally, simulation analysis and experimental test results show that the measurement accuracy and response performance of the proposed algorithm are better than that of the traditional algorithm and the corresponding commercial synchronous phasor measuring device in both steady state and dynamic state, and meet the practical application requirements.

Keywords: New energy grid · Phasor measurement · Discrete Fourier transform · Adaptive phasor algorithm

1 Introduction

With the large-scale development and utilization of renewable energy and the development of smart power grid, China has now built a super-large and complex interconnected power system [1]. It has the highest level of transmission voltage and

accommodates the largest amount of renewable energy in the world, and poses a great risk for safe operation [2]. Large-scale renewable energy that used to grid introduced a number of inverter, inverter, unified power flow controller of new power electronic equipment [3]. In the power system of power supply, power grid and load each link has obvious power electronic characteristics, cause subsynchronous oscillation disturbance phenomenon such as more frequent, presents the trend of the broadband domain grid harmonic interference, therefore improve the monitoring ability of power grid disturbance of different frequency components, reduce the risk of power grid operation [4]. In recent years, the wide area measurement system (WAMS) based on the synchronous phasor measurement device (PMU) has been widely used in the fields of power system dynamic process monitoring, online identification, security and stability analysis and wide area control [5]. With the deepening of WAMS application research, PMU requires more and more synchronous phasor measurement, and the accuracy and rapidity of its phasor algorithm will directly affect the reliability of related application functions [6].

At present, scholars at home and abroad have put forward a variety of synchronous phasor measurement algorithms, including discrete Fourier transform (DFT) method, dynamic phasor method, wavelet transform method, digital filter method and so on [7]. Among them, DFT algorithm is widely used because of its fast computation speed and strong harmonic suppression ability [8]. Literature [9] proposed a DFT calculation results are modified phasor measurement algorithm, compared with traditional DFT algorithm, the algorithm significantly improves the calculation precision, such as dynamic process response speed is limited, but for mutations and simplify the process done approximation is bigger, when great moment, amplitude changes in the frequency deviation meets the requirement of accuracy [10]. Recently, literature [11] proposed an algorithm based on the frequency domain dynamic model, which used the response of different frequency point filters of the same data window to modify the DFT estimation results, and improved the response speed of dynamic processes such as mutation. To solve the problem of weak noise suppression ability and low accuracy in fault process, literature [12] further proposes phasor algorithm using time-frequency information, which gives consideration to accuracy and speed requirements to some extent, but they do not give the method of frequency and harmonic suppression. As for the actual PMU, the PMU from the major manufacturers in China and the relevant test results abroad also show that the phasor algorithm used in various kinds of devices is still insufficient in the application range and practicability [13].

In view of the above problems, this paper also considers the speed and accuracy requirements of PMU algorithm, and proposes a comprehensive adaptive phasor algorithm: (1) improve the time domain algorithm, propose the use of Taylor series expansion to solve the original approximate processing problem, so as to significantly improve the accuracy of phasor measurement, still meet the national standard and IEEE standard requirements when the frequency deviation is large; (2) an improved frequency-domain algorithm is proposed to calculate the phasor, frequency and frequency change rate by calculating the fundamental wave and harmonic content on a data window. A kind of adaptive switching logic is proposed, which takes into account the calculation accuracy of steady state and the dynamic performance of transient state. By referring to the test methods given by national standards and IEEE standards, the

advantages of the proposed algorithm over the traditional DFT and the algorithm proposed in literature [9, 11] are verified through simulation. Furthermore, the physical experiment platform was used to test the measurement performance of the actual PMU developed based on the algorithm in this paper, and the measurement accuracy and response performance of the PMU under dynamic conditions were comprehensively compared with that of a mainstream commercial PMU.

2 Signal Modeling

Considering that the amplitude and phase Angle of the dynamic power signal may change with time, this paper adopts the complex signal to represent the dynamic phasor of the power signal. The power signal can be expressed as:

$$P(t) = a(t)e^{j\theta(t)} \quad (1)$$

$$x(t) = P(t)e^{j2\pi f_0 t} + P^*(t)e^{-j2\pi f_0 t} \quad (2)$$

Where, $a(t)$ and $\theta(t)$ represent the polynomials of the amplitude and phase Angle of the power signal respectively, f_0 is the rated frequency, $*$ and represents the conjugate.

The steady-state calculation mode uses the first-order model, assuming that the amplitude and frequency deviation are constant in the calculation period, that is: $a(t) = a$, $\theta(t) = \theta_0 + \theta_1 t$, Where a , θ_0 , θ_1 are respectively polynomial coefficients of amplitude and phase Angle. According to the specific accuracy requirements, the Taylor series expansion is simplified, and the DFT results of two adjacent data Windows are modified, with less computation and strong harmonic suppression ability, which meets the steady-state accuracy requirements.

In the dynamic calculation mode, it is assumed that the amplitude and phase Angle in the phasor model are k -order models (K is a natural number, in special case $K = 0$, corresponding to the traditional DFT algorithm), that is $a(t) = \sum_{i=0}^K a_i t^i$, $\theta(t) = \sum_{i=0}^K \theta_i t^i$. This can better reflect the dynamic characteristics of the signal. The phasor, frequency and frequency change rate are calculated by the fundamental wave and harmonic content of a data window, so as to meet the requirement of fast response of dynamic process.

3 Algorithm Synthesis Implementation

3.1 Time Domain Algorithm

In the steady-state computing mode, the original approximate processing problem is solved by the time-domain algorithm and the Taylor series expansion. Specifically, the discrete signal model is obtained by sampling formula (2) at N points every period, and the DFT transformation of the signal model is carried out. In this paper, the rectangular window is selected. Thus, the phasor of the power signal can be obtained as:

$$X = a_c e^{j\theta_c} = a e^{j\theta_0} e^{-\frac{j\theta_1(N-1)}{2Nf_0}} A(1 + e^{-jC} B) \quad (3)$$

$$\begin{cases} A = \frac{1}{N} \sin\left(\frac{\theta_1}{2f_0}\right) / \sin\left(\frac{\theta_1}{2Nf_0}\right) \\ B = \sin\left(\frac{\theta_1}{2Nf_0}\right) / \sin\left(\frac{\theta_1 + 4\pi f_0}{2Nf_0}\right) \\ C = 2\theta_0 + (\theta_1 + 2\pi f_0)(N - 1)/(Nf_0) \end{cases} \quad (4)$$

Where, a_c and θ_c respectively represent the calculated amplitude and phase Angle of DFT before correction.

To solve the problem that the approximate error of traditional DFT correction algorithm is large, the time domain algorithm proposed in this paper controls the error by expanding the Taylor series. To be specific, the error requirements under strict conditions of national standard and IEEE standard are considered comprehensively. In the process of approximate derivation, the approximate error should be within the order of 10^{-5} and below. Taking the approximation of B as an example, the Taylor series in the numerator and denominator are expanded to order 1 and order 3 respectively and simplified. As shown in Eq. (5), in the adverse case of sampling at 32 points per cycle and frequency deviation within 5 Hz, the maximum error after simplification is 1.5×10^{-6} , which is acceptable.

$$B \approx \frac{3N^2\theta_1}{4\pi(3N^2 - 2\pi^2)f_0 + (3N^2 - 6\pi^2)\theta_1} \quad (5)$$

Simplify A and $1 + e^{-jC}B$ by following a similar principle. On this basis, the relationship between the phasor after correction and the direct calculation of the phasor by DFT before correction can be obtained as follows:

$$a \approx \frac{a_c}{\frac{24f_0^2 - \theta_1^2}{24f_0^2} \sqrt{1 + B^2 + 2B \cos C}} \quad (6)$$

$$\theta_0 \approx \theta_c + D - \frac{\theta_1(N - 1)}{2Nf_0} \quad (7)$$

Where: $D = B \sin C / (1 + B \cos C)$

The Taylor series expansion of formula (7) can be obtained as follows:

$$\frac{D}{B} \approx F + GD + \frac{2}{3}GD^3 - \frac{4}{3}FD^4 \quad (8)$$

Where: $F = \sin(2\theta_c - 2\pi/N)$, $G = \cos(2\theta_c - 2\pi/N)$.

Under the same adverse circumstances, the error after the elimination of the higher order term is acceptable, and the approximate D is substituted into Eq. (7). The data window with k points is calculated like DFT, and the quadratic equation with one variable about B is obtained by combining with the assumed signal model, and then θ_1 is obtained. Substitute θ_1 into Eq. (7) to obtain the corrected phase Angle; The

amplitude of a after correction is obtained by formula (6). The corrected frequency is $f = f_0 + \theta_1/(2\pi)$. Finally, the phasor and frequency are smoothed according to the corrected frequency.

3.2 Frequency Domain Algorithm

Aiming at algorithms in the literature [11] gave no spectrum and frequency variation, and the harmonic interference when unable to obtain the phasor problem correctly, this article proposed frequency-domain algorithm and Taylor series expansion of the power signal model, and through a data window base wave frequency and frequency variation and phasor calculation, harmonic content, can be in a data window to calculate the frequency and frequency variation, and solve the problem of containing harmonic cases phasor calculation. Specifically, formula (1) is expanded into the form of real part and imaginary part of order K through Taylor series:

$$P(t) = \sum_{k=0}^K R_k t^k + j \sum_{k=0}^K I_k t^k = R(t) + jI(t) \tag{9}$$

Available:

$$\begin{cases} a_0 & = & \sqrt{R_0^2 + I_0^2} \\ \tan \theta_0 & = & \frac{I_0}{R_0} \\ \theta_1 & = & \frac{R_0 I_1 - R_1 I_0}{R_0^2 + I_0^2} \\ \theta_2 & = & \frac{R_0 I_2 - R_2 I_0}{R_0^2 + I_0^2} + \frac{(R_0 I_1 + R_1 I_0)(R_1 I_0 - R_0 I_1)}{(R_0^2 + I_0^2)^2} \end{cases} \tag{10}$$

By sampling at N points every period of formula (2), the signal model is discretized, and then DFT with coefficient of $e^{-jg_k \frac{2\pi n}{N}}$, where g_k is the set variable, is carried out after the signal model is windowed. In this paper, a rectangular window is selected, and the complex domain equation is:

$$\begin{aligned} x_k &= \frac{1}{N} \sum_{n=0}^{N-1} (P(n)e^{j\frac{2\pi n}{N}} + P^*(n)e^{-j\frac{2\pi n}{N}})e^{-jg_k \frac{2\pi n}{N}} \\ &= \frac{2}{N} \sum_{n=0}^{N-1} (\bar{R}(n) \cos \frac{2\pi n}{N} + \bar{I}(n) \sin \frac{2\pi n}{N})e^{-jg_k \frac{2\pi n}{N}} \end{aligned} \tag{11}$$

Where: X_k is the calculation result of the K times Fourier transform;

$$\bar{R}(n) = \sum_{k=0}^K \bar{R}_k n^k, \bar{I}(n) = \sum_{k=0}^K \bar{I}_k n^k, \text{ where, } \bar{R}_k = R_k / (Nf_0)^k, \bar{I}_k = I_k / (Nf_0)^k.$$

Expand the complex domain equation into the form of real part and imaginary part:

$$X_k = \frac{2}{N} M_k P \tag{12}$$

Where, $X_k = [X_{kR}, X_{kI}]^T$ is the vector formed by the real part X_{kR} and the imaginary part X_{kI} of the K times Fourier transform calculation result; $M_k = [M_{k0}, M_{k1}, \dots, M_{kK}]$ is the coefficient of the system, and its element expression is shown in Eq. (13). $P = [\bar{R}_0, \bar{I}_0, \bar{R}_1, \bar{I}_1, \dots, \bar{R}_K, \bar{I}_K]^T$ is the signal model parameter.

$$M_{ki} = \begin{bmatrix} \sum_{n=0}^{N-1} n^i \cos \frac{2\pi n}{N} \cos \frac{2\pi n g_k}{N} & - \sum_{n=0}^{N-1} n^i \sin \frac{2\pi n}{N} \cos \frac{2\pi n g_k}{N} \\ - \sum_{n=0}^{N-1} n^i \cos \frac{2\pi n}{N} \sin \frac{2\pi n g_k}{N} & \sum_{n=0}^{N-1} n^i \sin \frac{2\pi n}{N} \sin \frac{2\pi n g_k}{N} \end{bmatrix} \quad (13)$$

When $k = 0, 1, \dots, K$ simultaneous equations, get:

$$X = \frac{2}{N} MP \quad (14)$$

Where: $X = [X_0^T, X_1^T, \dots, X_K^T]^T$, $M = [M_0^T, M_1^T, \dots, M_K^T]^T$.

It should be noted that the selection of g_k in DFT coefficient should make the matrix M^{-1} condition number as small as possible to avoid ill-condition. At the same time, the power system harmonic interference should be suppressed. In order to suppress the common odd harmonic interference, 1,2,4..., that is, find the fundamental wave and the 2nd and 4th harmonic content of power signal in a data window. Since g_k can be determined in advance, the matrix M and its inverse M^{-1} can be calculated offline. In combination with Eq. (10) and (14), the amplitude at the calculation point is a_0 and the phase Angle is θ_0 . When the order K is ≥ 1 , the frequency deviation is $\theta_1/2\pi$. When $K \geq 2$, the rate of frequency change can be obtained as θ_2/π .

Theoretically, the higher the order K is, the higher the accuracy will be. However, in practical application, the higher the order K is, the higher the requirement for PMU software and hardware resources will be. Therefore, in engineering application, it is necessary to select according to the actual situation.

3.3 Verification Algorithm and Comprehensive Algorithm Implementation

In view of the problem that the existing algorithm can not take into account both the calculation accuracy of steady state and the dynamic performance of transient state, the algorithm proposed in this paper can realize the adaptive switching of calculation mode through verification under different conditions, so as to take into account the requirements of fast response and high precision.

Specifically, by calculating the phasor, the theoretical calculated values of each sampling point are deduced, and compared with the actual measured points. If the total deviation is small, the test passes. For example, for the time-domain algorithm, the theoretical calculation value of each extraction point is deduced from θ_0 , θ_1 and a after correction, and the density of the extraction point is determined according to the actual situation:

$$x_c(n_i) = a \cos(\theta_0 + \frac{n_i\theta_1}{Nf_0} + \frac{2\pi n_i}{N}) \tag{15}$$

Where: $n_i(i = 1, 2, \dots, L)$ is the selected point, and $1 \leq n_i \leq N$, where L is the total number of samples; $x_c(n_i)$ is the theoretical value of the extracted point.

The total deviation between the theoretical calculated value and the measured value is:

$$\varepsilon = \sum_{i=1}^L |x_c(n_i) - x_m(n_i)| \tag{16}$$

Where: $x_m(n_i)$ is the measured value of the corresponding sampling point.

The overall flow of the comprehensive algorithm is shown in Fig. 1, mainly including the following steps: (1) assume that the power signal is a first-order model, solve the phasor through the time domain algorithm; (2) through the comparison of the back value and the measured value, check the calculation result is correct, if the check through, the end, if not, it means that the current may be in a sudden change and other dynamic process, into the next step; Assuming that the power signal is a k-order model, the phasor, frequency and frequency change rate are solved by frequency domain algorithm. (4) check whether the calculation results of the frequency-domain algorithm are correct. If the calibration fails, the failure may occur in the case that the equal-frequency algorithm in this data window is also unable to deal with. In order to avoid large fluctuations, the results of the time-domain algorithm are still used.

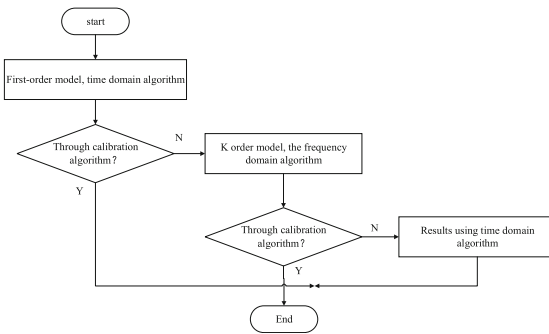


Fig. 1. Comprehensive phasor measurement algorithm to achieve the flow

4 Simulation Analysis

The national standard and IEEE standard specify the measurement method and precision requirement of PMU under steady state and dynamic condition in detail. According to the reference standards in literature [14], devices of four major PMU manufacturers in China were tested, and the test results showed that all four failed to fully meet the standard requirements, and some indicators even had a large deviation.

In this paper, the performance of the algorithm was comprehensively tested and analyzed by reference to the standard in MATLAB, and compared with the traditional DFT algorithm (algorithm 1), the DFT correction algorithm (algorithm 2) proposed in literature [9], and the DFT correction algorithm (algorithm 3) proposed in literature [11] using the response of different frequency point filters. Due to the limitation of space, the steady-state performance and the dynamic performance of the step response under the three important indexes of frequency deviation, harmonic influence and frequency linear change are analyzed emphatically in this paper. In the simulation process, the sampling frequency of each algorithm is equal to 6400 Hz, and the interval between two adjacent data Windows in the time-domain algorithm in this paper is 64 points. The phasor model of the frequency-domain algorithm adopts the third-order model.

4.1 Frequency Deviation Analysis

When the frequency deviation is 5 Hz, the corresponding maximum error, average absolute error and root mean square error of each algorithm are shown in Table 1. It can be seen that when the frequency deviates from the rated frequency, the error of algorithm 1 and 2 is large. The measurement accuracy of this algorithm is high and meets the requirements of national standards. The reason is that the unsynchronized sampling of algorithm 1 leads to the spectrum leakage, and algorithm 2 makes a large approximation in the process of simplification. However, under the premise of ensuring the accuracy, the algorithm in this paper deduces the approximation by controlling the number of Taylor series expansion terms, so the accuracy is high.

Table 1. Error of each algorithm when frequency deviation is 5 Hz

Algorithm	Angle error (°)			Amplitude error (%)		
	Maximum	Mean absolute	Root mean square	Maximum	Mean absolute	Root mean square
1	20.5899	17.9382	18.0240	-5.2690	2.6560	3.0882
2	-5.7974	3.5874	3.9897	-1.6936	1.1305	1.2126
3	-3.009	0.1444	0.1801	-0.4.89	0.1927	0.2416
This paper	-0.0022	0.0009	0.0012	0.0072	0.0071	0.0071

4.2 Harmonic Influence Analysis

According to the national standard, the algorithms are analyzed under the frequency deviation of 0.5 Hz and the superposition of 2–13 harmonics of rated amplitude of 20%. The simulation results are shown in Table 2. It can be seen from Table 2 that when the frequency is shifted by 0.5 Hz with serious harmonic interference, the error of algorithm 3 is large. The accuracy of the algorithm in this paper is better than that of algorithm 1 and 2, and it meets the requirements of the latest national standard. Due to the limitation of the signal model and algorithm principle of algorithm 3, the

fundamental phasor of the power signal cannot be acquired correctly. In this paper, the harmonic suppression capability of DFT algorithm is integrated, and the frequency deviation is high precision.

Table 2. Error of each algorithm under harmonic influence

Algorithm	Angle error (°)			Amplitude error (%)		
	Maximum	Mean absolute	Root mean square	Maximum	Mean absolute	Root mean square
1	2.4059	1.7921	1.8334	3.831	0.444	0.777
2	-2.0174	0.4138	0.5425	3.777	0.395	0.747
3	178.9468	40.0514	55.2037	210.990	49.748	62.768
This paper	0.0040	0.0015	0.0016	-0.005	0.002	0.000

4.3 Frequency Slope Response Analysis

According to IEEE standard, the slope test signal with frequency deviation of 5 Hz and rate of change of 1 Hz/s is applied to test the accuracy of each algorithm. The mathematical expression of the input signal is as follows:

$$x(t) = a \cos(2\pi f_0 t + 2\pi \Delta f t + \pi t^2 + \pi/2) \quad (17)$$

When a is equal to 1, it's equal to 50 Hz. The error results of each algorithm are shown in Table 3. It can be seen that when the signal frequency range is wide and the frequency linear change is fast, the algorithm in this paper still maintains high accuracy and is better than the other three algorithms. Among them, the maximum frequency error is 0.001 Hz and the maximum frequency change rate error is 0.0088 Hz/s, which all meet the requirements of IEEE standard.

Table 3. Error of each algorithm during ramp change of frequency

Algorithm	Angle error (°)			Amplitude error (%)		
	Maximum	Mean absolute	Root mean square	Maximum	Mean absolute	Root mean square
1	21.7653	18.6971	18.7951	-5.63	2.71	3.18
2	-6.1125	3.7240	4.1378	-1.89	1.23	1.32
3	-0.3546	0.1637	0.2042	-0.48	0.22	0.27
This paper	0.0537	0.0446	0.0449	-0.01	0.01	0.01

4.4 Step Response Analysis

In order to test the response performance of the algorithm to dynamic processes such as mutation, 90° phase Angle step signal was applied according to the national standard:

$$x(t) = \begin{cases} a \cos(2\pi f_0 t + \pi/6) & t < 40 \text{ ms} \\ a \cos(2\pi f_0 t + \pi/6 + \pi/2) & t \geq 40 \text{ ms} \end{cases} \quad (18)$$

The step response curves of each algorithm are shown in Fig. 2.

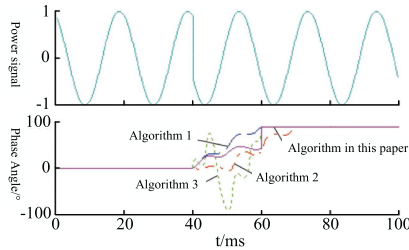


Fig. 2. Step response curves of each algorithm

According to the definition of response time by the national standard, the response time of the algorithm in this paper is about 20 ms, which is faster than algorithm 2 (30 ms) and has higher accuracy than algorithm 3. This is because the algorithm in this paper ADAPTS to the frequency domain algorithm after the step response, and only needs one period of data. Algorithm 2 needs two data Windows, so the algorithm in this paper has a faster response speed than algorithm 2, while algorithm 3 fluctuates greatly in the data window where the fault is due to the limitation of principle. At the same time, it also shows the correctness of the proposed algorithm.

5 Experimental Test

Based on the embedded software and hardware platform, PMU is developed. The developed PMU converts large voltage and current signals into small voltage signals through voltage and current transformers. Then, according to the global positioning system’s second pulse, the voltage signals are sampled at regular intervals in time synchronization through 16-bit analog digital converter, and the sampled signals are processed in the digital signal processor chip. The experimental test platform used for this test is shown in Fig. 3.

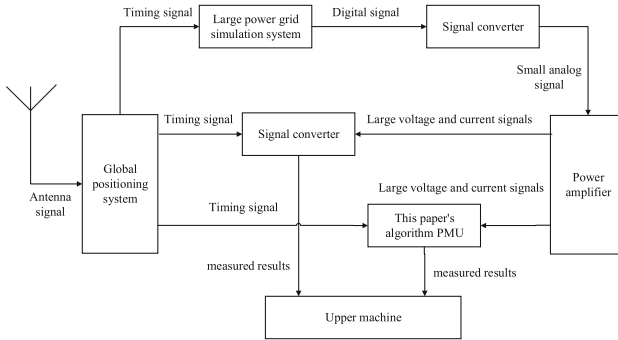


Fig. 3. PMU test system

5.1 Measurement Accuracy Test Under Dynamic Condition

The curve of comparing the voltage amplitude of the slave node measured by commercial PMU and the PMU algorithm in this paper with the truth value is shown in Fig. 4(a). The truth value refers to the data directly sent from the simulation system. By calculation, the average absolute error of the amplitude of commercial PMU is 0.17%, while the algorithm in this paper is 0.14%. Figure 4(b) shows the curve comparing the relative phase Angle measured by the commercial PMU and the PMU algorithm in this paper with the true value. By calculation, the average absolute error of the phase Angle of the commercial PMU is 0.156° , while the algorithm in this paper is 0.062° . According to Fig. 4 and the calculation error, in the dynamic process, both PMUs meet the requirements of the national standard. The algorithm in this paper is closer to the truth value than the commercial PMUs, but due to the limitation of hardware conditions, the accuracy improvement level is not significant.

5.2 Fast Response Performance Test Under Dynamic Conditions

In order to objectively compare the response performance of the commercial PMU and the algorithm in this paper under dynamic conditions, 34 short-circuit simulation experiments were carried out in succession. The test results show that the phasor cannot be measured correctly 16 times in the short circuit process of the commercial PMU, and the algorithms in this paper are all normal. Figure 5(a) shows the curve of amplitude and truth value comparison of slave stations measured by commercial PMU and the algorithm in this paper. Figure 5(b) shows the curve of relative phase Angle and true

value of the horizontal leach-derived station measured by commercial PMU and the algorithm in this paper. It can be seen that in the short-circuit process, the commercial PMU has a point with amplitude of 0 and a large fluctuation of relative phase Angle, which is not consistent with the true value, indicating that the algorithm in this paper has a faster response performance than the commercial PMU in some transient processes.

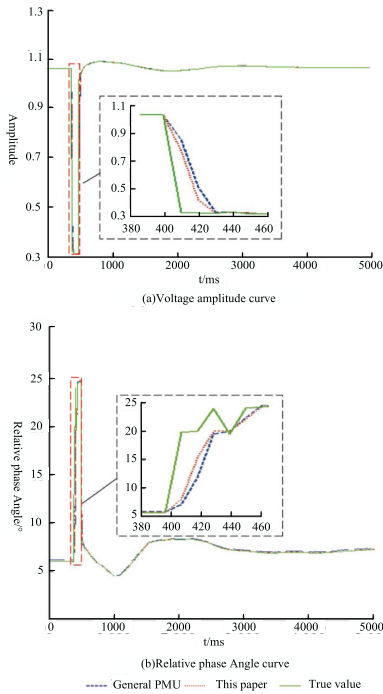


Fig. 4. Curves of voltage magnitude and angle

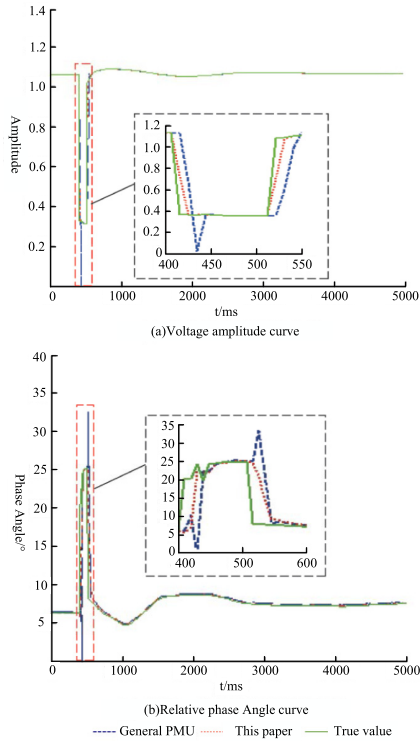


Fig. 5. Curves of voltage magnitude and angle under quick response performance testing

6 Conclusion

In this paper, a comprehensive adaptive phasor algorithm based on Taylor series and DFT is proposed. According to the national standard and IEEE standard, the proposed algorithm is comprehensively simulated in MATLAB. Based on the algorithm in this paper, PMU is implemented and compared with a mainstream commercial PMU on a digital - physical hybrid simulation platform. Theoretical simulation and experimental test results show that the proposed algorithm has superior performance, mainly in the following aspects.

- 1) in the steady-state calculation mode, time-domain algorithm is adopted to simplify the calculation by Taylor series expansion under the premise of analysis to ensure the accuracy, which has high accuracy and strong harmonic suppression ability.
- 2) in the dynamic computing mode, the frequency domain algorithm is adopted to calculate the amplitude, phase Angle, frequency and frequency change rate only through the fundamental wave and each harmonic content of a data window, with fast response speed and harmonic suppression ability.

- 3) through the calculation of the phasor, the strategy of reversely deducing the theoretical calculation value of each sampling point and comparing it with the measured value can be adopted to switch the calculation mode adaptively, taking into account the accuracy and rapidity requirements.
- 4) the implementation, accuracy and fast response performance of the actual PMU are better than the commercial PMU compared, indicating that the proposed algorithm can meet the requirements of practical application.

Acknowledgement. This work was supported by Natural Science Foundation of Liaoning Province (2019-MS-239).

References

1. Imdadullah, S., Amrr, M.: A comprehensive review of power flow controllers in interconnected power system networks. *IEEE Access* **26**(8), 18036–18063 (2020)
2. Liu, B.: An AC–DC hybrid multi-port energy router with coordinated control and energy management strategies. *IEEE Access* **24**(7), 109069–109082 (2019)
3. Pegoraro, P., Brady, K., Castello, P.: Compensation of systematic measurement errors in a pmu-based monitoring system for electric distribution grids. *IEEE Trans. Instrum. Meas.* **68**(10), 3871–3882 (2019)
4. Narduzzi, C., Bertocco, M., Frigo, G.: Fast-TFM—multifrequency phasor measurement for distribution networks. *IEEE Trans. Instrum. Meas.* **67**(8), 1825–1835 (2018)
5. Zhao, J., Zhang, G., Jabr, R.: Robust detection of cyber attacks on state estimators using phasor measurements. *IEEE Trans. Power Syst.* **32**(3), 2468–2470 (2017)
6. Moghimi, M., Xu, W.: Online determination of external network models using synchronized phasor data. *IEEE Trans. Smart Grid* **9**(2), 635–643 (2018)
7. Kabiri, M., Amjady, N.: A new hybrid state estimation considering different accuracy levels of pmu and scada measurements. *IEEE Trans. Instrum. Meas.* **68**(9), 3078–3089 (2019)
8. Sun, L.: Optimum placement of phasor measurement units in power systems. *IEEE Trans. Instrum. Meas.* **68**(2), 421–429 (2019)
9. Wang, M., Sun, Y.: A DFT-based method for phasor and power measurement in power systems. *Autom. Electric Power Syst.* **29**(2), 20–24 (2005)
10. Koteswara, A., Soni, K., Sinha, S.: Accurate phasor and frequency estimation during power system oscillations using least squares. *IET Sci. Meas. Technol.* **13**(7), 989–994 (2019)
11. Fu, L., Han, W.: Dynamic phasor estimator based on frequency-domain model. *Proc. CSEE* **35**(6), 1371–1378 (2015)
12. Jain, S., Singh, N.: A fast harmonic phasor measurement method for smart grid applications. *IEEE Trans. Smart Grid* **8**(1), 493–502 (2017)
13. Fernandes, E.: Application of a phasor-only state estimator to a large power system using real PMU Data. *IEEE Trans. Power Syst.* **32**(1), 411–420 (2017)